Swelling-induced surface instability of a hydrogen-bonded LBL film and its self-healing

Qiuyan Han [a], Chong Li [a], Ying Guan [a], X.X. Zhu [b], Yongjun Zhang [a],*

[a] State Key Laboratory of Medicinal Chemical Biology and Key Laboratory of Functional Polymer Materials, Institute of Polymer Chemistry, College of Chemistry, Nankai University, and Collaborative Innovation Center of Chemical Science and Engineering (Tianjin), Tianjin 300071, China
[b] Department of Chemistry, Université de Montréal, C.P. 6128, Succursale Centre-Ville, Montreal, QC H3C 3J7, Canada

ABSTRACT

Thin hydrogel films attached to a rigid substrate can only swell along the direction perpendicular to the substrate, which generates compressive stress within the gel. When the stress is sufficiently large, the free surface of the gel will locally buckle and fold against itself to form various wrinkling patterns. Here we show that hydrogen-bonded layer-by-layer (LBL) films of poly(vinyl pyrrolidone) (PVPON) and poly(acrylic acid) (PAA) also swell in ethanol/water mixtures. Like ordinary hydrogel films attached to a substrate, the LBL films also undergo mechanical instability when their swelling degree is large enough. By adjusting the composition and pH of the ethanol/water mixture, the swelling degree of the film can be adjusted, which further decides whether the mechanical instability occurs or not. Like ordinary hydrogel films, the surface wrinkling of the PVPON/PAA films occurs via a nucleation-growth process. Unlike ordinary hydrogels, the critical swelling degree for the onset of wrinkling for PVPON/PAA films increases with increasing film thickness. More importantly, the wrinkling patterns can be healed automatically, because the transient network of PVPON/PAA films allows for the relief of compressive stress via its rearrangement. The phenomenon observed here may provide a possible way to erase the undesired wrinkling patterns on constrained hydrogel films.

© 2014 Elsevier Ltd. All rights reserved.

1. Introduction

Hydrogels are crosslinked 3D networks of hydrophilic polymer chains which swell but do not dissolve in solvents [1]. To exploit their applications such as cell culture substrata [2], sensor coatings [1], etc, they are frequently engineered as thin films attached on a rigid substrate. The gel films swell when immersed in water. As they are mechanically confined by the substrate, they can only expand along the direction normal to the substrate. The anisotropic swelling generates in-plane compressive stress within the gel. When the stress is sufficiently large, the free surface of the gel will locally buckle and fold against itself to form various wrinkling patterns [3] (Scheme 1A). Swelling-induced mechanical instability has been observed from various hydrogels, such as polyacrylamide (PAAm) [4,5], poly(N-isopropylacrylamide) (PNIPAM) [6–8], and poly(2-hydroxyethyl methacrylate) (PHEMA) [9,10]. In many cases the swelling-induced mechanical instability is undesired and

should be avoided. Therefore this instability places a fundamental limit on the degree to which a gel can swell while remaining flat [5]. However, the wrinkling patterns can also be harnessed for various advanced applications [11–14].

In recent years numerous ultrathin hydrogel-like membranes were fabricated using the so-called layer-by-layer (LBL) assembly method [15]. In LBL assembly, two polymers with complementary functional groups are deposited onto a substrate in a layer-by-layer manner, using various interactions, such as electrostatic interaction, hydrogen bonding [16,17], and covalent bonding, as the driving forces [18]. Through this method, thin films with finely controlled thickness can be easily coated on substrates of any shape. These films have found a wide range of potential applications, such as salt separation, drug release, and biosensing [19–22]. In many cases the films will contact with a solvent and may undergo significant swelling. As they are usually attached on a rigid substrate, one may expect that they may also experience swelling-induced surface wrinkling. Like ordinary hydrogel films, the swelling-induced instability will pose barriers for the application of LBL films.

In this contribution, the swelling-induced mechanical instability of hydrogen-bonded LBL films of poly(vinyl pyrrolidone) (PVPON)
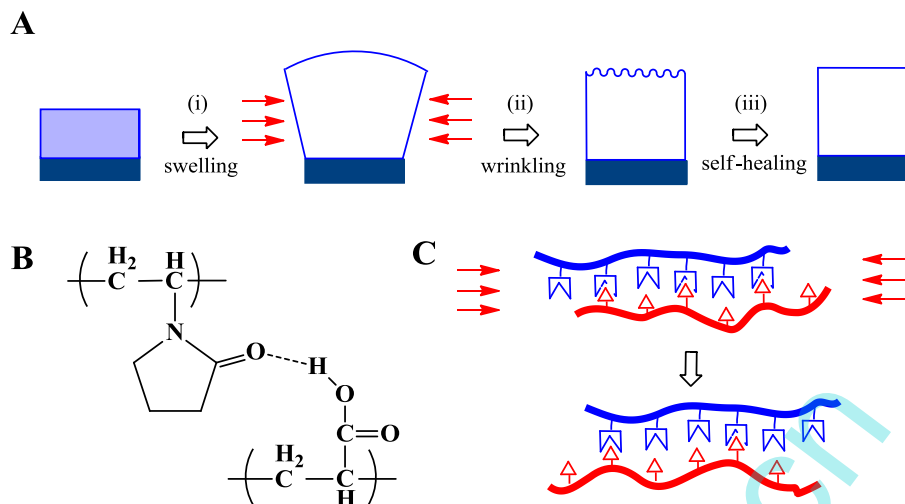
Scheme 1. (A) Swelling-induced wrinkling and its self-healing of PVPON/PAA LBL film: (i) Like ordinary substrate-attached hydrogel film, anisotropic swelling results in equibiaxial compressive stress within the film [4]. (ii) The film surface buckles when the stress is above a critical threshold. (iii) The transient network of PVPON/PAA film allows for the relief of the compressive stress and the wrinkles are self-healed. (B) Dynamic hydrogen bonding between PVPON and PAA in the PVPON/PAA LBL films. (C) A schematical illustration of the relief of the compressive stress via the rearrangement of the transient network.

and poly(acrylic acid) (PAA) in ethanol/water mixtures was investigated. The purpose of the present study is twofold. Firstly we want to examine if an LBL film undergoes swelling-induced mechanical instability like ordinary substrate-attached hydrogel films as expected. We found the film surface remains flat at a low swelling degree, but develops wrinkling patterns when its swelling is larger than a critical degree. Secondly we want to examine if the swelling-induced wrinkling patterns can be healed automatically via the rearrangement of the dynamic network of the film (Scheme 1A). Unlike ordinary hydrogels crosslinked with permanent covalent bonds, the PVPON/PAA films are crosslinked via reversible hydrogen bonds. Their network is transient and dynamic in nature [23,24], which endows them self-healing ability like other dynamic hydrogels crosslinked with reversible bonds [25–27]. Although a lot of experimental and theoretical studies have been carried out to understand the swelling-induced instability of substrate-attached gel films [28,29], to the best of our knowledge, no method has been proposed to heal the undesired wrinkling patterns.

2. Experimental section

2.1. Materials

Poly(vinyl pyrrolidone) (PVPON) (MW 100 000) and poly(acrylic acid) (PAA) (MW 10 000) were purchased from Sigma–Aldrich. Other chemicals are all of analytical grade. The chemicals were used as received without further purification.

2.2. Film fabrication

The PVPON/PAA LBL films were fabricated as reported previously [30,31]. Briefly, silicon wafers, used as substrate, were cleaned in boiling piranha solution (3:7 v/v H_2O_2–H_2SO_4 mixture) (*caution: this solution is extremely corrosive!*) before use. The pH of the PVPON and PAA solutions were adjusted to 3.0 with 0.1 M HCl. The silicon wafers were then dipped into a 0.1 wt% PVPON solution and a 0.1 wt% PAA solution alternately, each for 4 min, washing in 10^{-3} M HCl for 1 min in between. After the desired number of dipping cycles was reached, the film was annealed in 10^{-3} M HCl for 6 h and then dried in the air. The resultant film is denoted as "(PVPON/PAA)$_n$",

which means the film is fabricated from PVPON and PAA and has n bilayers.

2.3. Morphology study

Ethanol/water mixtures were prepared by mixing predetermined amount of ethanol and deionized (DI) water. The composition of the mixtures is expressed as the volume percent concentration (v/v %) of ethanol. In certain cases, the pH of water was first adjusted using HCl and then mixed with ethanol. The surface morphology of the LBL films immersed in the solvents was observed using an Olympus BX51 optical microscope. Images were captured by a digital camera coupled with the microscope. All experiments were carried out at room temperature ($\sim$23 °C).

2.4. Other characterizations

The reflection spectra of the films were measured with an AvaSpec-2048 Fiber Optic spectrometer. An experimental setup reported previously [32] was used when the films were immersed in solvents. In this setup, temperature of the sample cell was controlled with a refrigerated circulator. Atomic force microscopy (AFM) images were acquired on a Benyuan CSPM5000s scanning probe microscope in tapping mode.

3. Results and discussion

3.1. Swelling of PVPON/PAA films in water

The PVPON/PAA LBL films were previously studied by several groups [30,31,33–35]. The films were assembled via the formation of hydrogen bonds between PVPON, as hydrogen acceptor, and PAA, as hydrogen donor (Scheme 1B) [30,33]. As they are actually a crosslinked network of PVPON and PAA, they can be regarded as hydrogels [15,32,36]. Like ordinary hydrogels, the PVPON/PAA films can also swell in water.

The swelling of PVPON/PAA films can be facilely studied using the Fabry–Perot fringes on their reflection spectra, providing that the film surfaces remain smooth during the process [30]. As shown in Fig. S1A in the supporting information, the reflection spectra of a (PVPON/PAA)$_{20}$ film, measured in air as dry film, display oscillations
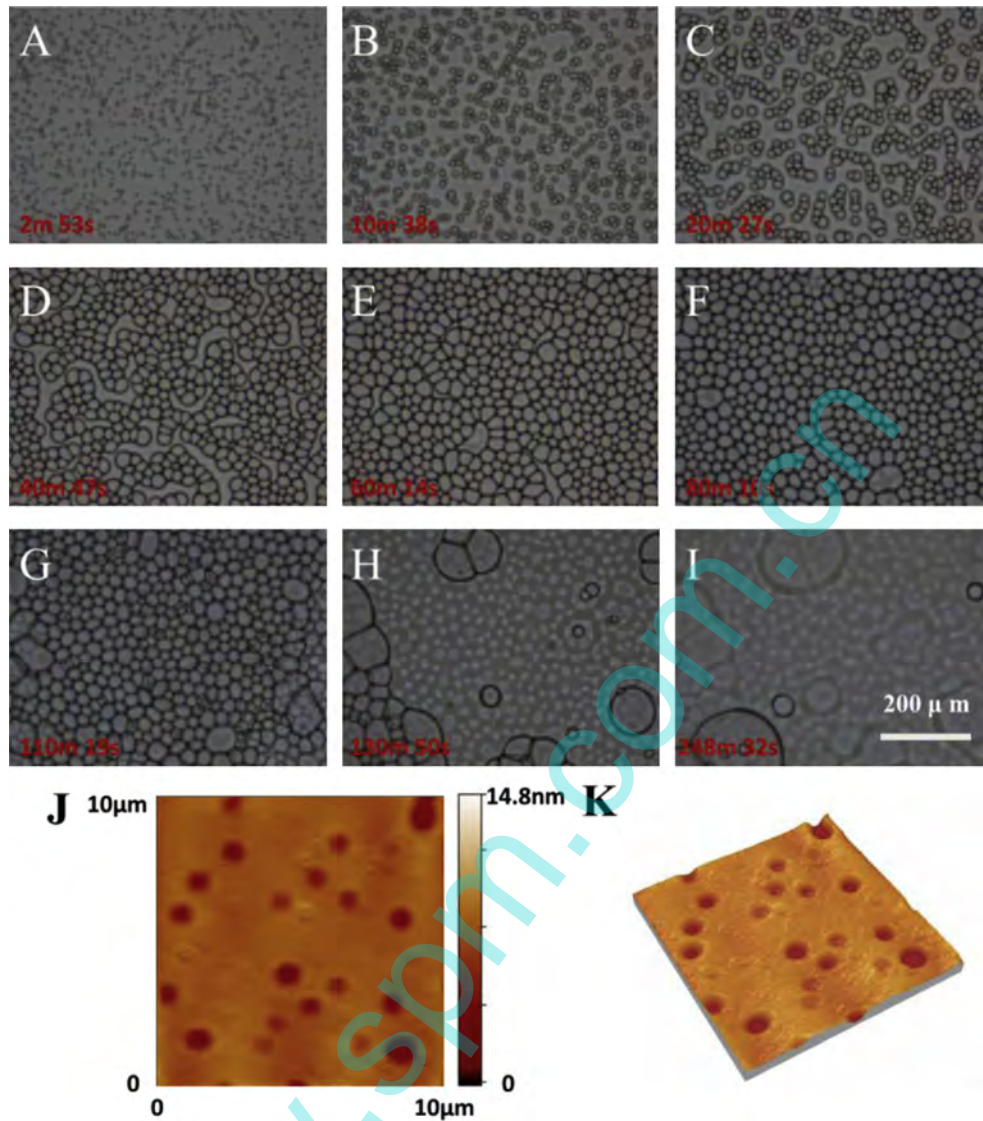
Fig. 1. (A–I) Time evolution of surface morphology of a (PVPON/PAA)$_{20}$ film soaking in 40% ethanol/water mixture. (J, K) AFM image of a (PVPON/PAA)$_{20}$ film after a brief immersion in 40% ethanol/water mixture.

known as Fabry–Perot fringes. These fringes originate from the interferences between beams reflected at the air-film and film–substrate interfaces (inset in Fig. S1A) [30,32,34]. From two adjacent peak wavelengths, λ_p and λ_{p+1}, the film thickness, h, can be calculated using the following relationship [30]:

$$h = \frac{1}{2n_e(1/\lambda_p - 1/\lambda_{p+1})} \tag{1}$$

where n_e is the refractive index of the film, which was previously measured to be 1.45 [30]. For the 20-bilayer film shown in Fig. S1A, its thickness was calculated to be ∼1440 nm. The reflection spectra of the same film immersed in water were also shown in Fig. S1A. Compared with the spectra measured in air as dry film, the amplitude of the oscillations is reduced significantly. When the film is transferred into water, the refractive index of the medium increases from 1.0 (air) to 1.33 (water), significantly reducing the difference in refractive index at the medium–film interface. Accordingly, the amount of light reflected at the interface decreases, resulting in a reduced amplitude of the Fabry–Perot fringes

[32]. Also using Eq. (1) and ignoring the slight decrease in refractive index of the film, the thickness of the wet film was calculated to be ∼1850 nm. The increased thickness indicates clearly that the film swells in water. The swelling degree of the film, SD, was calculated to be ∼1.28 using the following equation:

$$SD = \frac{h_s}{h_0} \tag{2}$$

where h_0 and h_s are the thicknesses of the dry and swollen film, respectively.

The swelling kinetics can also be easily monitored using the same method. As shown in Fig. S1B, once immersed in water, the film swells quickly. The swelling equilibrium is attained within 5 s. The extremely quick swelling of the PVPON/PAA film is attributed to its thin thickness, as the swelling rate of a hydrogel is inversely proportional to the square of its characteristic dimension [37].

The morphology change of the film during swelling was examined using an optical microscope. The original dry film is highly smooth as reported previously [30,31] and it remains highly

smooth in water. No coarsening of the film surface was observed. In addition, well-defined Fabry–Perot fringes were observed throughout the swelling process. It is known that Fabry–Perot fringes can only be observed from highly smooth films [30,31]. This observation confirms again that the film remains flat and smooth during its swelling in water.

3.2. Surface wrinkling in ethanol/water mixtures

The above experiments reveal that the PVPON/PAA film swells in water like ordinary hydrogels, however, no swelling-induced instability was observed in the experimental time-frame, possibly because its swelling degree in water is not large enough. Although both PVPON and PAA are highly hydrophilic, the film material, which is actually an interpolymer complex [38], is somewhat hydrophobic. Therefore its swelling degree in water is relatively low.

An enhanced swelling of PVPON/PAA film can be achieved by adding ethanol to water. In this way, significant surface wrinkling was observed. As a typical example, Fig. 1 shows the morphology changes of a $(PVPON/PAA)_{20}$ film immersed in 40 v/v% ethanol/water mixture. The original dry film is highly smooth without any features on the surface. Shortly after immersion in the ethanol/water mixture, however, small round features were generated on the film surface (Fig. 1A). AFM imaging shows these features are shallow holes surrounded with a raised rim, looking like craters (Fig. 1J and K). These features grow gradually with time and coalesce with the neighboring features (Fig. 1B–G). At an extended immersion, the wrinkling patterns fade gradually (Fig. 1H and I).

Besides the 40% ethanol/water mixture, the morphology changes of $(PVPON/PAA)_{20}$ films in ethanol/water mixtures with various compositions were studied. Typical results were collected in Fig. 2. Similar surface wrinkling was observed in 60% ethanol/water mixture, but the film remains largely flat in 20% and 80% ethanol/water mixtures. The results suggest that the PVPON/PAA film behaves differently in solvents with different composition.

The mechanical instability of substrate-attached hydrogel films in solvents has been explained by their anisotropic swelling [4,5,9,10]. Unlike free-standing films which can swell uniformly in all directions, a substrate-attached gel can only expand in the direction normal to the substrate, because of the mechanical constraint provided by the rigid substrate. The uniaxial swelling of the gel results in equibiaxial compressive stress within the film [4,5]. When this compressive stress becomes sufficiently large, the free surface of the gel folds upon itself to locally relieve the compressive stress (Scheme 1A).

A prerequisite for the wrinkling of the gel surface is that the swelling degree of the gel is large enough to produce sufficiently large compressive stress [3]. Previous theoretical and experimental studies indicate that the onset of wrinkling is only related to the effective compressive strain experienced by the surface layer, irrespective of the modulus and thickness of the mismatched layers [13]. The critical value of compressive strain for wrinkling instability, ε_c, was reported to be 0.35 [13]. For the critical swelling ratio, Kang and Huang's theoretical and numerical analyses found it lies between 2.5 and 3.4 [29], while Dervaux and Ben Amar [28] found it lies between 1.5 and 3, depending on the underlying mechanism of volume variation. Recently, Hayward et al. [5] established that the critical swelling degree for the onset of wrinkling of surface-bound PAAm hydrogel films, expressed as film thickness change ratio, is ∼2. This value is in excellent agreement with Biot's theoretical predictions [39]. However, Guvendiren et al. [10] found that, for their PHEMA hydrogel films with depth-wise crosslinking gradient, the onset of wrinkling is at a linear expansion of ∼1.12.

The different behaviors of the PVPON/PAA film in different solvents are expected to originate from the different swelling degree of the film. As shown above, the swelling degree of PVPON/PAA film in pure water is only ∼1.28. This value should be smaller than the critical swelling degree for the onset of wrinkling, therefore the film remains flat. We tried to use Fabry–Perot fringes to measure the swelling degree of PVPON/PAA film in ethanol/water mixtures. Unfortunately, because of the occurrence of surface wrinkling, the Fabry–Perot fringes always become ill-defined, or even disappear totally, especially in 40% and 60% ethanol/water mixtures. To circumvent this difficulty, we used mixtures of ethanol and 10^{-3} M HCl, instead of mixtures of ethanol and pure water. In ethanol/10^{-3} M HCl mixtures, Fabry–Perot fringes can still be clearly observed from the reflection spectra of the film, thus allowing for the measurement of swelling degree.

As shown in Fig. S2 in the supporting information, the equilibrium swelling degree, SD_e, of the film first increases gradually with increasing ethanol concentration in the solvent, reaches a maximum at 60% ethanol, and then drops sharply with further increasing ethanol concentration. The SD_es at 60% and 40% ethanol, which are the highest and the second highest, are ∼1.90 and ∼1.74, respectively. It is expected that in ethanol/water mixture the same trend will be followed. In addition the SD_e of PVPON/PAA films should be larger in ethanol/water than in ethanol/10^{-3} M HCl. Therefore, it is likely that the SD_e of the film in 40% and 60% ethanol/water mixtures will be higher than the critical swelling degree for the onset of wrinkling (∼2 as suggested by Hayward et al. [5]). As a result, mechanical instability of the film was observed in the two solvents. In contrast, the SD_e of the film in 20% and 80% ethanol/water mixtures should be still lower than the critical swelling degree, therefore, the film remains largely flat in these solvents.

The swelling degree of the PVPON/PAA film can not only be influenced by the composition of the ethanol/water mixture, but also by its pH. For the SD_e of $(PVPON/PAA)_{20}$ films in water, it decreases from ∼1.28 in DI water (pH∼5.5) to ∼1.23 in water with pH3.0. A lower pH suppresses the deprotonation of the carboxylic acid groups in PAA, and thus reduces the swelling degree of the film [40,41]. A lower pH should reduce the SD_e of PVPON/PAA film in ethanol/water mixtures in a similar manner.

To study the effect of pH, a series of mixtures were prepared by mixing ethanol with water whose pH was adjusted using HCl. Ethanol concentrations of the mixtures are all at 60%. It is noteworthy that the pH5.5 mixture is actually prepared using "pure" water without adding HCl. Fig. 3 shows the patterns developed on $(PVPON/PAA)_{20}$ film surface after 10 min immersion in the
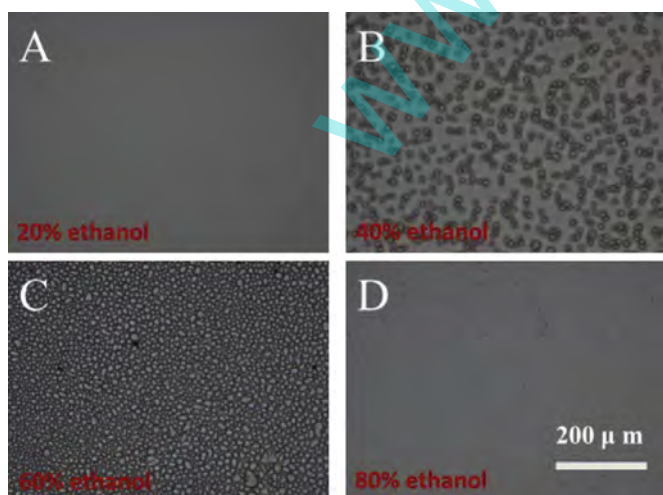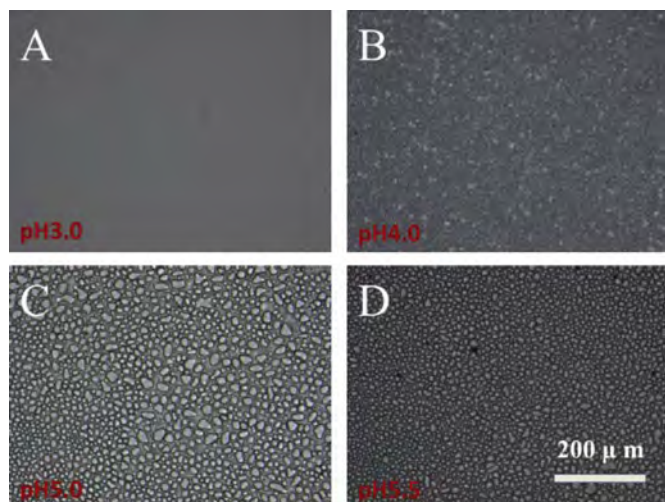

Fig. 2. Morphology of $(PVPON/PAA)_{20}$ films after soaked in ethanol/water mixtures for 10 min. Ethanol concentration is 20%(A), 40%(B), 60%(C), and 80%(D), respectively.

Fig. 3. Surface morphology of (PVPON/PAA)$_{20}$ films after soaked in 60% ethanol/water mixtures for 10 min. pH is 3.0(A), 4.0(B), 5.0(C), and 5.5(D), respectively.

mixtures. In mixtures with a pH of 4.0—5.5, obvious surface wrinkling was observed, but the film remains flat in pH3 mixture. The results suggest that the swelling of the film is suppressed to a large extent at pH3, resulting in a swelling below the critical swelling degree for the onset of wrinkling. In contrast, the swelling at pHs 4.0 and 5.0 is less suppressed and is still higher than the critical swelling degree, therefore surface instability was observed at these pHs.

In the previous studies, 20-bilayer films with a thickness around 1500 nm were used. To study the effect of film thickness on their behavior in ethanol/water mixture, PVPON/PAA films with various bilayer numbers were fabricated. They were then treated with 60% ethanol/water mixture. Surface wrinkling was observed from all 4 films (Fig. 4), suggesting the swelling of the films is all higher than the critical swelling degree for the onset of wrinkling.

3.3. Nucleation, growth, and coalescence of the wrinkling patterns

Previous studies reveal that the swelling-induced surface instability of substrate-attached hydrogels may occur through a
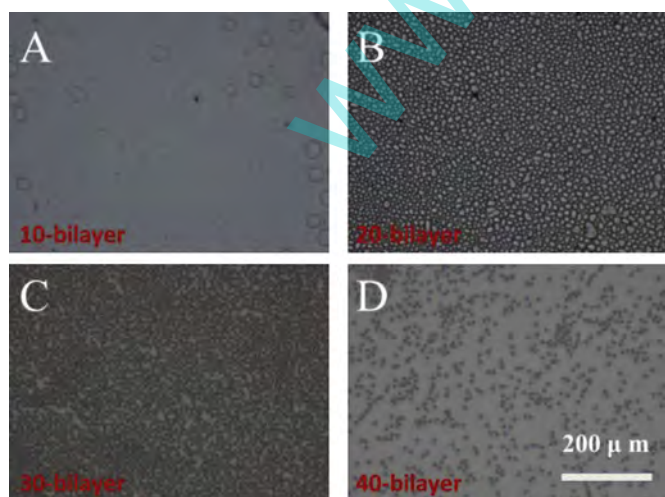
Fig. 4. Morphology of 10(A), 20(B), 30(C), and 40-bilayer (D) PVPON/PAA films after being soaked in 60% ethanol/water mixture for ∼10 min.

linear instability, or via a nucleation-growth process [10,13]. Particularly Hayward et al. [7] studied the formation of surface creases on PNIPAM copolymer gel layers and found creases appear through the formation of short nuclei that grow laterally across the surface. Close examination of the buckling process of the PVPON/PAA film reveals also a nucleation-growth process. The pattern evolution on the 20-bilayer film in 40% ethanol/water mixture is a typical example (Fig. 1). The round wrinkling features with a size ∼2 μm were first observed at an immersion time of 40 s. Thereafter these features grow gradually. We calculated the number of the features and found it decreases monotonously with time (Fig. S3 in the supporting information). In addition we did not observe the emergence of any new features at the later stage of the process. These observations suggest the nucleation process only occurs at the very early stage, probably shortly after the swelling of the film overpasses the critical swelling degree for the onset of wrinkling. It is well-known that many structures form via a nucleation-growth mechanism and the separation of nucleation and growth stage always results in monodispersed structures [42]. In deed the wrinkling features obtained here are rather uniform in size, especially before their coalescence. The narrow size distribution of the features also suggests that the stress field, as a result of the rapid swelling of the film, is uniform [43].

Fig. 5 shows a typical example of the growth process of the wrinkling features. The driving force for the continuous growth of these features is considered to be the residual stresses in the unbuckled areas [43]. Particular attention was paid to the growth of single features, such as the one indicated in Fig. 5. Fig. 6 shows the size change of several separated features with time. We only examined the cases in which the density of the wrinkling features is low which allows for the examination of single features.

As shown in Fig. 6, the size of the features increases continuously with time. Previously the growth kinetics of wrinkling pattern of constrained hydrogels was studied by several groups [7,10,44]. In these studies, for the early stage of pattern evolution, the relationship between the size of the pattern, expressed by its characteristic wavelength, λ, and time t was found to be $\lambda(t) \propto t^{1/2}$. As shown in Fig. 6, a linear relationship between the pattern size and $t^{1/2}$ was also found for the early stage of pattern growth. By extrapolating to a pattern size of 0, the time for the first emergence of the wrinkling pattern can be determined, which is ∼10 s for all three cases shown in Fig. 6. Previously Guvendiren et al. [10] reported that an induction period of ∼2 min was necessary for the pattern to develop on their PHEMA hydrogel films. Compared with Guvendiren et al.'s hydrogel films, the initiation of surface buckling of PVPON/PAA films is much faster, possibly due to the fast swelling of these thin films (see Fig. S1B).

The features grow gradually into contact with each other, and coalesce to form larger features. This is the main reason for the decreasing feature number with time as shown in Fig. S3. As an example, Fig. S4 shows the process of the coalescence of adjacent wrinkling features. Coalescence of two adjacent round features results in an oval-shaped feature. Interestingly, the oval-shaped feature becomes round-shaped gradually, suggesting the residual stress the feature experienced is isotropic.

The nucleation-growth mechanism allows for a deeper analysis of the wrinkling pattern process. For the (PVPON/PAA)$_{20}$ films, it is expected that a larger degree of swelling will generate more wrinkling nuclei at the nucleation stage. For example, the swelling degree of the film is larger in 60% mixture than in 40% mixture, therefore immersion in 60% mixture produces more wrinkling features. Because of their large amount, these features coalesce quickly to afford larger features with irregular shape as shown in
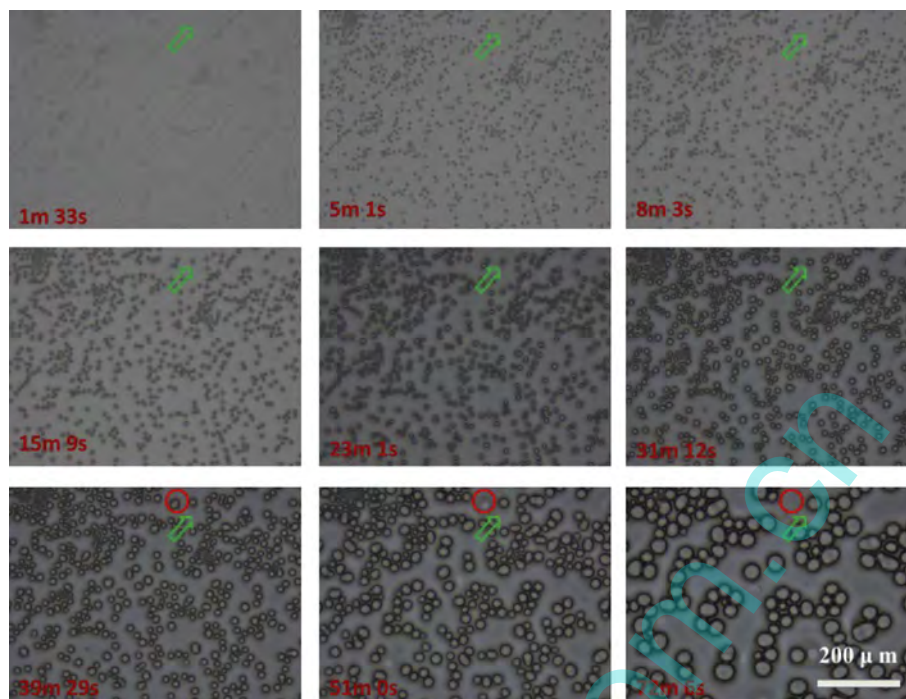
Fig. 5. Time evolution of surface morphology of a 40 bilayer PVPON/PAA film soaking in 60% ethanol/water mixture. Green arrow indicates the gradual expansion of a single feature with time. Red circle indicates the disappearance of a feature. (For interpretation of the references to color in this figure legend, the reader is referred to the web version of this article.)

Fig. 2C. Similarly the swelling degree of the (PVPON/PAA)$_{20}$ film decreases when the pH of the 60% ethanol/water mixture decreases from 5.5 to 4. The amount of wrinkling nuclei generates at the nucleation stage decreases accordingly, giving the different wrinkling patterns at different pHs as shown in Fig. 3.

The swelling degree of films with different thickness in the same 60% ethanol/water mixture is expected to be the same, therefore one may expect that same amount of wrinkling nuclei will generate and hence similar wrinkling pattern will appear on films with different thicknesses. Surprisingly images shown in Fig. 4 imply that the amount of wrinkling nuclei generates at the nucleation stage actually increases with decreasing film thickness. Particularly because of a very large number of wrinkling nuclei generate at the nucleation stage and their quick coalescence and self-healing (see

below), the wrinkling pattern of the thinnest (PVPON/PAA)$_{10}$ film at an immersion time of ∼10 min, as shown in Fig. 4A, is already partially self-healed.

To explain this phenomenon we examined the critical ethanol concentration for the onset of wrinkling. These films were treated with ethanol/water mixtures with various ethanol concentrations. As shown in Fig. 7, the critical ethanol concentration for the onset of wrinkling decreases with decreasing film thickness, from ∼44% ethanol for a 40 bilayer film to ∼33% ethanol for a 10 bilayer film. Therefore when the films are all immersed in 60% ethanol/water mixture, a larger compressive stress and hence more wrinkling nuclei will generate within a thinner film. As the swelling degree of PVPON/PAA film increases with increasing ethanol concentration in this range of ethanol concentration (see Fig. S2), the results shown in Fig. 7 suggest the critical swelling degree for the onset of wrinkling increases with increasing film thickness. Previous studies on ordinary hydrogels reveal that the critical strain for surface buckling is relatively insensitive to the thickness of the gel [5,7]. In this respect, the behavior of the PVPON/PAA films is different from ordinary hydrogels.
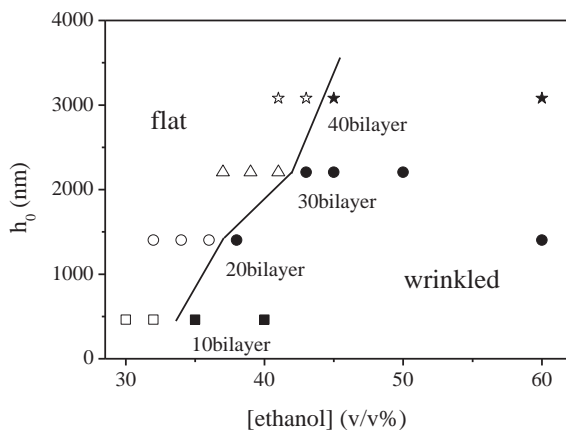
3.4. Self-healing of wrinkling patterns

We have shown that the PVPON/PAA LBL films undergo surface wrinkling in ethanol/water mixtures when their swelling degree is large enough, similar to ordinary surface-attached hydrogel films. Previous studies on ordinary hydrogels showed that the growth of wrinkling pattern will finally stop and a permanent pattern will be obtained because the mechanical constraint of the substrate is permanent [4,44]. Some wrinkling patterns remain stable even after drying [9].

In contrast, we observed the disappearance of the wrinkling features from the PVPON/PAA films. As shown in Fig. 8, the feature indicated by arrow continues to grow until an immersion time of
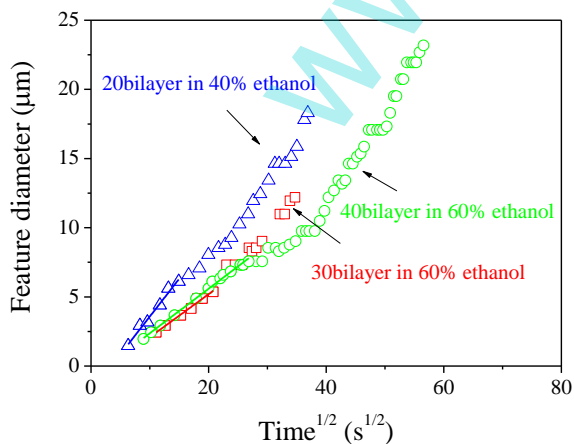
Fig. 6. Size change of single features with time. (□) a (PVPON/PAA)$_{30}$ film immersed in 60% ethanol/water mixture. (○) a (PVPON/PAA)$_{40}$ film immersed in 60% ethanol/water mixture. (△) a (PVPON/PAA)$_{20}$ film immersed in 40% ethanol/water mixture.

Fig. 7. Stability diagram of PVPON/PAA films with different thickness in ethanol/water mixtures. Open symbols indicate the film remains flat while the solid ones indicate mechanical instability occurs.
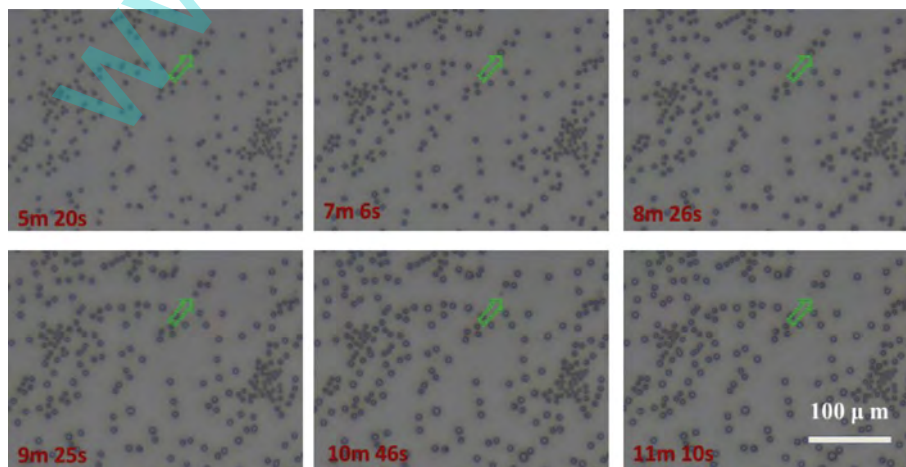
is mechanically constrained by the inner part. Similarly mechanical instability occurs when the swelling degree of the surface layer is large enough. When the gel is fully swollen, however, the surface layer is no longer mechanically constrained. With the relief of compressive stress, the flat gel surface is restored.

Here the relief of compressive stress in PVPON/PAA films is achieved via a different way. Unlike ordinary hydrogels which are crosslinked with covalent bonds, in the PVPON/PAA films the PVPON chains bind with PAA chains via reversible hydrogen bonds (Scheme 1B). Therefore the 3D network of the film is transient. The crosslinks can be broken and reform again and are at a dynamic equilibrium between breakage and formation. Hydrogels cross-linked with similar reversible/dynamic bonds were usually referred as dynamic hydrogels [25–27,45–48]. It was reported that the transient network of dynamic hydrogels can be broken when applied a large strain, but recover upon the removal of the strain [26]. Here the dynamic nature of the PVPON/PAA film allows it to relief the compressive stress via the rearrangement of the network (Scheme 1C). As a result the wrinkling pattern can be self-healed. In contrast for ordinary surface-contrained hydrogels, as their cross-links are permanent and will not allow for rearrangement, the wrinkling pattern will not vanish.

4. Conclusions

In conclusion, we demonstrate that the PVPON/PAA LBL films behave similar to ordinary surface-attached hydrogels. They swell in ethanol/water mixtures. In addition, they undergo mechanical instability when their swelling degree is larger than a critical degree, because the film is mechanically constrained by the rigid substrate and can only swell in direction perpendicular to the surface. The swelling-induced surface wrinkling of LBL films certainly will pose barriers for some of their applications where the film surface is required to remain flat in solvent.

The PVPON/PAA LBL films also display behaviors different from ordinary hydrogels. Particularly the swelling-induced buckling of ordinary constrained hydrogels results in permanent wrinkling patterns. In contrast, the dynamic network of the PVPON/PAA film allows for the relief of compressive stress and therefore the wrinkling pattern can be healed automatically. Base on this observation, we expect that novel hydrogel films capable of self-healing the undesired wrinkling patterns will be designed by introducing dynamic crosslinks.

~9 min. Thereafter it begins to shrink and finally vanishes. It is noteworthy this is not an isolated case. Another example can be found from the images shown in Fig. 5.

Because the wrinkling features vanish gradually, the film surface becomes less coarse after an extended immersion. A typical example was shown in Fig. 1. The result indicates that the swelling-induced surface instability is partially self-healed. A more pronounced example was observed when immersing a 20 bilayer PVPON/PAA film in pH4 60% ethanol/water mixture. As shown in Fig. 9, surface coarsening of the film was observed shortly after the immersion. The film surface is first fully covered with fine wrinkling features. With time elapses, the wrinkling features grow to a bigger size, however, their number drops sharply, leaving more and more film surface unbuckled. Finally the whole surface becomes flat again.

As mentioned above, the film surface buckles because of the swelling-induced compressive stress, and the residual stresses in the unbuckled surface drives the wrinkling features to grow with time. [43] The disappearance of the wrinkling features suggest the local residual compressive stress in the film is relieved. Previously wrinkling patterns was also observed from **unconstrained** hydrogels at their early stage of swelling [4]. At this stage, the surface layer is swollen, but the inner part is not, therefore the surface layer

Fig. 8. Surface morphology of a 40 bilayer PVPON/PAA film immersed in 60% ethanol/water mixture. The wrinkling feature indicated by arrow first grows with time and then vanishes.
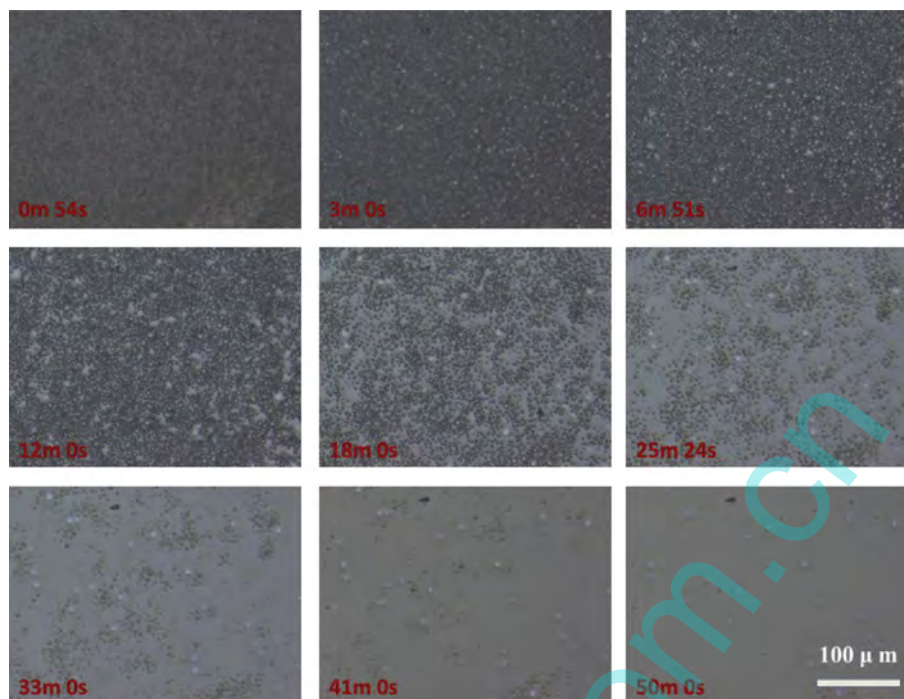
Fig. 9. Surface morphology of a 20 bilayer PVPON/PAA film immersed in pH4 60% ethanol/water mixture.

Acknowledgments

Appendix A. Supplementary data

Supplementary data related to this article can be found online at http://dx.doi.org/10.1016/j.polymer.2014.03.015.

References

[1] Buenger D, Topuz F, Groll J. Prog Polym Sci 2012;37(12):1678—719.
[2] Cooperstein MA, Canavan HE. Langmuir 2010;26(11):7695—707.
[3] Dervaux J, Ben Amar M. Annu Rev Condens Matter Phys 2012;3:311—32.
[4] Tanaka T, Sun S, Hirokawa Y, Katayama S, Kucera J, Hirose Y, et al. Nature 1987;325(6107):796—8.
[5] Trujillo V, Kim J, Hayward RC. Soft Matter 2008;4(3):564—9.
[6] Ortiz O, Vidyasagar A, Wang J, Toomey R. Langmuir 2010;26(22):17489—94.
[7] Yoon J, Kim J, Hayward RC. Soft Matter 2010;6(22):5807—16.
[8] Kim J, Yoon J, Hayward RC. Nat Mater 2010;9(2):159—64.
[9] Guvendiren M, Yang S, Burdick JA. Adv Funct Mater 2009;19(19):3038—45.
[10] Guvendiren M, Burdick JA, Yang S. Soft Matter 2010;6(9):2044—9.
[11] Yang S, Khare K, Lin P. Adv Funct Mater 2010;20(16):2550—64.
[12] Li B, Cao Y, Feng X, Gao H. Soft Matter 2012;8(21):5728—45.
[13] Arifuzzaman M, Wu ZL, Kurokawa T, Kakugo A, Gong JP. Soft Matter 2012;8(31):8060—6.
[14] Yang Y, Han X, Ding W, Jiang S, Cao Y, Lu C. Langmuir 2013;29(23):7170—7.
[15] Kozlovskaya V, Kharlampieva E, Erel I, Sukhishvili SA. Soft Matter 2009;5(21): 4077—87.
[16] Wang L, Wang Z, Zhang X, Shen J, Chi L, Fuchs H. Macromol Rapid Commun 1997;18(6):509—14.
[17] Stockton WB, Rubner MF. Macromolecules 1997;30(9):2717—25.
[18] Zhang X, Chen H, Zhang HY. Chem Commun 2007;14:1395—405.
[19] Tong W, Song X, Gao C. Chem Soc Rev 2012;41(18):6103—24.
[20] Matsusaki M, Ajiro H, Kida T, Serizawa T, Akashi M. Adv Mater 2012;24(4): 454—74.
[21] Wohl BM, Engbersen JFJ. J Control Release 2012;158(1):2—14.
[22] Such GK, Johnston A, Caruso F. Chem Soc Rev 2011;40(1):19—29.
[23] Zhang X, Guan Y, Zhang Y. J Mater Chem 2012;22(32):16299—305.
[24] Zhou L, Chen M, Tian L, Guan Y, Zhang Y. ACS Appl Mater Interf 2013;5(9): 3541—8.
[25] Deng G, Tang C, Li F, Jiang H, Chen Y. Macromolecules 2010;43(3):1191—4.
[26] He L, Fullenkamp DE, Rivera JG, Messersmith PB. Chem Commun 2011;47(26): 7497—9.
[27] Zhang Y, Yang B, Zhang X, Xu L, Tao L, Li S, et al. Chem Commun 2012;48(74): 9305—7.
[28] Dervaux J, Ben Amar M. J Mech Phys Solids 2011;59(3):538—60.
[29] Kang MK, Huang R. J Mech Phys Solids 2010;58(10):1582—98.
[30] Guan Y, Yang SG, Zhang YJ, Xu J, Han CC, Kotov NA. J Phys Chem B 2006;110(27):13484—90.
[31] Lin W, Guan Y, Zhang YJ, Xu J, Zhu XX. Soft Matter 2009;5(4):860—7.
[32] Zhang X, Guan Y, Zhang Y. Biomacromolecules 2012;13(1):92—7.
[33] Sukhishvili SA, Granick S. Macromolecules 2002;35(1):301—10.
[34] Zhang W, Zhang A, Guan Y, Zhang Y, Zhu XX. J Mater Chem 2011;21(2):548—55.
[35] Zhang W, Song J, Liao W, Guan Y, Zhang Y, Zhu XX. J Mater Chem C 2013;1(10):2036—43.
[36] Ding ZB, Guan Y, Zhang YJ, Zhu XX. Polymer 2009;50(17):4205—11.
[37] Tanaka T, Fillmore DJ. J Chem Phys 1979;70(3):1214—8.
[38] Lau C, Mi YL. Polymer 2002;43(3):823—9.
[39] Biot MA. Appl Sci Res A 1963;12(2):168—82.
[40] Jones CD, Lyon LA. Macromolecules 2000;33(22):8301—6.
[41] Zhang YJ, Guan Y, Zhou SQ. Biomacromolecules 2006;7(11):3196—201.
[42] Sugimoto T. Chem Eng Tech 2003;26(3):313—21.
[43] Sharp JS, Jones RAL. Phys Rev E 2002;66:11801.
[44] Tanaka H, Tomita H, Takasu A, Hayashi T, Nishi T. Phys Rev Lett 1992;68(18): 2794—7.
[45] Guan Y, Zhang Y. Chem Soc Rev 2013;42(20):8106—21.
[46] Tuncaboylu DC, Argun A, Algi MP, Okay O. Polymer 2013;54(23):6381—8.
[47] Zeng F, Han Y, Yan Z, Liu C, Chen C. Polymer 2013;54(26):6929—35.
[48] Tuncaboylu DC, Argun A, Sahin M, Sari M, Okay O. Polymer 2012;53(24): 5513—22.